EM Manifold Estimation of GNSS Synchronization Parameters Under Constant Modulus Interference

Asmae Bendahmane, *University of Toulouse, ENAC*
Alexandre Brochard, *University of Toulouse, ISAE-SUPAERO/ENAC*
Julien Lesouple, *University of Toulouse, ENAC*
Lorenzo Ortega, *IPSA/TéSA*
Jordi Vilà-Valls, *University of Toulouse, ISAE-SUPAERO*

***Abstract*—Global Navigation Satellite Systems (GNSS) rely on estimating the signal propagation delay and Doppler shift to a set of visible satellites, which in turn allows to determine the receiver position, velocity and timing. However, the presence of interfering signals degrades the estimation of such synchronization parameters, reason why robust solutions must be accounted for. Considering constant modulus (CM) interferences, which include chirp and continuous wave signals, a recent solution proposed an expectation-maximization (EM) algorithm to estimate both interference and signal parameters, which relies on the von Mises distribution to exploit the interference CM property. In this contribution, we exploit the geometric properties of the CM family using a Riemannian framework, where CM interferences are modeled as a Riemannian manifold. This modeling allows the E-step of the EM algorithm to be replaced by a Riemannian gradient descent over that manifold. Results show that the proposed method improves the estimation performance and reduces the complexity compared to the classical EM approach.**

***Keywords*—Expectation maximization, Riemannian manifold optimization, GNSS, constant modulus interference.**

I. Introduction

It is well known that Global Navigation Satellite Systems (GNSS) are vulnerable to a variety of non-nominal propagation conditions, threats and attacks, and in particular to interference sources (i.e., either intentional or unintentional). Therefore, interference mitigation techniques are essential in safety critical applications for reliable positioning. [1], [2]. Indeed, GNSS signals received power is roughly -159 dBW [3], which implies that these signals are deeply buried under the noise floor, making them particularly susceptible to interference.

A particularly effective interference mitigation strategy is to resort to antenna arrays, which allow to implement beamforming or null-steering methods [4], but this is of limited applicability for small platforms or low-cost mass-market receivers. For single antenna receivers, a variety of techniques have been proposed in the literature, where interference can be mitigated at various stages [5]. Most of the traditional techniques are applied before the correlation step, including pulse blanking [6], where samples exceeding a fixed energy threshold are set to zero, and notch filtering [7], where the jammer's frequency is tracked and removed from the received signal. Recent approaches resort to spectral estimation [8], deep neural networks [9] or robust statistics [10], [11]. In contrast, the method recently presented in [12], [13] exploits a parametric statistical model for constant modulus (CM) interferences, and consider an expectation-maximization (EM) algorithm to estimate both GNSS parameters and interference.

In this article, we focus on the EM approach, an iterative algorithm consisting of two steps: 1) the E-step can be interpreted as the estimation of the statistical mean of the interference, which is then subtracted from the received signal to isolate a cleaner GNSS signal; 2) the M-step involves estimating the corresponding delay and Doppler using a classical maximum likelihood estimator (MLE). These two steps are repeated iteratively until convergence. But in the E-step, the mean vector does not necessarily preserve the CM property.

CM interferences exhibit a specific geometric structure, represented as a product of unit circles, which can be leveraged to improve the synchronization parameters estimation through manifold optimization. In [14], Riemannian optimization was applied to an array signal processing problem under a CM constraint, where the interference mitigation problem was modeled as a constrained minimization task, and the CM property was embedded within the Riemannian manifold framework. The goal was to exploit the CM property on the reflection coefficient of the array. In this contribution, we further explore the approach in [12], [13] and propose to replace the E-step of the EM algorithm, designed for GNSS CM interference mitigation, with a Riemannian optimization over the manifold of CM interferences. This ensures that the estimated interference preserves the CM property, leading to a more robust solution compared to the classical one.

II. Signal model

We consider a system where a band-limited signal $s(t)$, with bandwidth B, is transmitted over a carrier frequency f_c (i.e., $\lambda_c = \frac{c}{f_c}$) from a transmitter T at position $\boldsymbol{p}_T(t)$ to a receiver R at position $\boldsymbol{p}_R(t)$. Assuming a first-order approximation, the T to R distance is given by

$$p_{TR} \approx c(\tau + bt), \tag{1}$$

where $\tau = \frac{\|\boldsymbol{p}_T(0) - \boldsymbol{p}_R(0)\|}{c}$ and $b = \frac{\|\boldsymbol{v}\|}{c}$, with $\boldsymbol{v}$ representing the relative velocity vector between the transmitter and receiver. Under the narrowband assumption and considering an interference $I(t)$ degrading the received signal, the baseband demodulated signal can be expressed as [15]:

$$x(t;\boldsymbol{\eta}) = \alpha s(t-\tau)e^{-j2\pi f_c(b(t-\tau))} + I(t) + n(t), \tag{2}$$

This work was partially supported by the DGA/AID project 2022.65.0082.

with $\boldsymbol{\eta} = (\tau, b)^\top$ and $\alpha = \rho e^{j\phi} \in \mathbb{C}$. Moreover, $n(t)$ represents an additive circularly symmetric complex Gaussian noise. Considering $N = N_2 - N_1 + 1$ samples at the sampling frequency $F_s = B = \frac{1}{T_s}$, the discrete vector signal model is

$$\boldsymbol{x} = \alpha \boldsymbol{\mu}(\boldsymbol{\eta}) + \boldsymbol{I} + \boldsymbol{n}, \tag{3}$$

with $\boldsymbol{x} = (\dots, x(kT_s), \dots)^\top$, $\boldsymbol{I} = (\dots, I(kT_s), \dots)^\top$ the interference samples, $\boldsymbol{n} = (\dots, n(kT_s), \dots)^\top \sim \mathcal{CN}(\boldsymbol{n}; \boldsymbol{0}, \sigma^2 I_N)$ the noise samples, with $N_1 \leq k \leq N_2$ and

$$\boldsymbol{\mu}(\boldsymbol{\eta}) = (\cdots, s(kT_s - \tau) e^{-j2\pi f_c b(kT_s - \tau)} \cdots)^\top \in \mathbb{C}^N, \tag{4}$$

the signal component. Under the CM interference, all the components of the vector $\boldsymbol{I}$ have the same modulus $A \geq 0$. Then, the interference $\boldsymbol{I}$ can be expressed as follows:

$$\boldsymbol{I} = A\tilde{\boldsymbol{I}}, \tag{5}$$

where $\tilde{\boldsymbol{I}} = (\cdots, \tilde{I}_k, \cdots)^\top$ with $\tilde{I}_k = e^{j\theta_k}$ and $|\tilde{I}_k| = 1$. Note that $\theta_k \in (0, 2\pi]$ and $\boldsymbol{\theta} = (\cdots, \theta_k, \cdots)^\top$, which means that $\tilde{\boldsymbol{I}}$ belongs to the complex hyper-torus of dimension N.

III. Maximum Likelihood Parameter Estimation via Expectation-Maximization

Assuming independent and identically distributed (i.i.d.) samples, the likelihood function can be written as [12], [13]

$$p(\boldsymbol{x}|\boldsymbol{\theta}, \boldsymbol{\varepsilon}) = \frac{1}{\pi^N \sigma^{2N}} e^{-\frac{1}{\sigma^2}(\boldsymbol{x} - \alpha\boldsymbol{\mu}(\boldsymbol{\eta}) - A\tilde{\boldsymbol{I}})^H (\boldsymbol{x} - \alpha\boldsymbol{\mu}(\boldsymbol{\eta}) - A\tilde{\boldsymbol{I}})}, \tag{6}$$

with $\boldsymbol{\varepsilon} = \{\boldsymbol{\eta}^\top, \rho, \phi, A, \sigma^2\}$ the vector of unknown deterministic parameters. To estimate the GNSS parameters of interest, gathered in $\boldsymbol{\eta}$, the MLE seeks to maximize (6). However, this maximization is intractable due to the unknown vector $\boldsymbol{\theta}$. A possible solution, as in [12], is to resort to the EM algorithm, which allows to approximate the MLE when latent variables are present. Then, we consider $\boldsymbol{\theta}$ as latent variables and we derive the so-called complete likelihood, which is the joint likelihood of the observed and latent random variables

$$\mathcal{L}_c(\boldsymbol{\varepsilon}; \boldsymbol{x}, \boldsymbol{\theta}) = p(\boldsymbol{x}, \boldsymbol{\theta}|\boldsymbol{\varepsilon}) = p(\boldsymbol{x}|\boldsymbol{\theta}, \boldsymbol{\varepsilon}) p(\boldsymbol{\theta}). \tag{7}$$

Considering independent uniform priors on $[0, 2\pi)$ for θ_k,

$$p(\boldsymbol{\theta}) = \prod_{i=1}^{N} \frac{1}{2\pi} 1_{[0,2\pi)}(\theta_k), \tag{8}$$

leading to the following complete likelihood expression,

$$\begin{aligned} \mathcal{L}_c(\boldsymbol{\varepsilon}; \boldsymbol{x}, \boldsymbol{\theta}) &\propto \frac{1}{\sigma^{2N}} e^{-\frac{1}{\sigma^2}(x - \alpha\boldsymbol{\mu}(\boldsymbol{\eta}) - A\tilde{\boldsymbol{I}})^H (x - \alpha\boldsymbol{\mu}(\boldsymbol{\eta}) - A\tilde{\boldsymbol{I}})} \\ &\propto \frac{e^{-\frac{1}{\sigma^2}(x - \alpha\boldsymbol{\mu}(\boldsymbol{\eta}))^H (x - \alpha\boldsymbol{\mu}(\boldsymbol{\eta})) - \frac{A^2 N}{\sigma^2} + \frac{2A}{\sigma^2}\mathrm{Re}\{\tilde{\boldsymbol{I}}^H (x - \alpha\boldsymbol{\mu}(\boldsymbol{\eta}))\}}}{\sigma^{2N}}, \end{aligned} \tag{9}$$

where $\mathrm{Re}\{\cdot\}$ is the real part operator. The EM algorithm consists of two steps: 1) the expectation E-step, where the likelihood to maximize is locally approximated by the expected value of the latent parameters $\boldsymbol{\theta}$, holding the parameters to be estimated fixed as $\boldsymbol{\varepsilon}^{(t)}$ (i.e., superscript (t) refers to the t-th algorithm iteration), and 2) the maximization M-step, where the parameters to estimate are updated by maximizing the approximation with respect to $\boldsymbol{\varepsilon}$. This process is iterated until convergence. In the E-step, the approximation is expressed as,

$$\begin{aligned} Q(\boldsymbol{\varepsilon}|\boldsymbol{\varepsilon}^{(t)}) = E_{\boldsymbol{\theta}|\boldsymbol{x}, \boldsymbol{\varepsilon}^{(t)}}[\log \mathcal{L}_c(\boldsymbol{\varepsilon}; \boldsymbol{x}, \boldsymbol{\theta})] = \frac{A^2}{\sigma^2} \left(\hat{\boldsymbol{I}}^{(t)}\right)^H \hat{\boldsymbol{I}}^{(t)} \\ - \frac{A^2}{\sigma^2} N + K' - N \log \sigma^2 - \frac{\left\| \boldsymbol{x} - \rho e^{j\phi} \boldsymbol{\mu}(\boldsymbol{\eta}) - A\hat{\boldsymbol{I}}^{(t)} \right\|^2}{\sigma^2}, \end{aligned} \tag{10}$$

where the conditional distribution $\theta_k|\boldsymbol{x}, \boldsymbol{\varepsilon}^{(t)}$, is a von Mises distribution with mean $\gamma_k^{(t)}$ and spread parameter $\kappa_k^{(t)}$ as

$$\gamma_k^{(t)} = \arg\left(x_k - \alpha^{(t)} \mu_k\left(\boldsymbol{\eta}^{(t)}\right)\right) \tag{11}$$

$$\kappa_k^{(t)} = \frac{2A^{(t)}}{(\sigma^{(t)})^2} \left| x_k - \alpha^{(t)} \mu_k\left(\boldsymbol{\eta}^{(t)}\right) \right| \tag{12}$$

where x_k, resp. $\mu_k\left(\boldsymbol{\eta}^{(t)}\right)$, is the k-th component of the vector $\boldsymbol{x}$, resp. $\boldsymbol{\mu}\left(\boldsymbol{\eta}^{(t)}\right)$. Moreover, $\hat{\boldsymbol{I}}^{(t)} = (\cdots, w_k^{(t)} e^{j\gamma_k^{(t)}}, \cdots)$ is the t-th iteration estimate of $\tilde{\boldsymbol{I}}$, with $w_k^{(t)} = \frac{I_1\left(\kappa_k^{(t)}\right)}{I_0\left(\kappa_k^{(t)}\right)}$ and I_p the modified Bessel function of the first kind and order p. The derivation of such expression can be found in [12]. The M-step updates the value of $\boldsymbol{\varepsilon}$ as

$$\boldsymbol{\varepsilon}^{(t+1)} = \arg\max_{\boldsymbol{\varepsilon}} Q(\boldsymbol{\varepsilon}|\boldsymbol{\varepsilon}^{(t)}). \tag{13}$$

Defining $\boldsymbol{U} = \left(\hat{\boldsymbol{I}}^{(t)}\right)^H \boldsymbol{\Pi}_{\boldsymbol{\mu}(\boldsymbol{\eta})}$ and $\boldsymbol{U}^\perp = \left(\hat{\boldsymbol{I}}^{(t)}\right)^H \boldsymbol{\Pi}^\perp_{\boldsymbol{\mu}(\boldsymbol{\eta})}$, yields (as it has been shown in [12])[1]

$$\boldsymbol{\eta}^{(t+1)} = \arg\max_{\boldsymbol{\eta}} \left\| \boldsymbol{\Pi}_{\boldsymbol{\mu}(\boldsymbol{\eta})} \left(\boldsymbol{x} - \frac{\mathrm{Re}\left\{\boldsymbol{U}^\perp \boldsymbol{x}\right\} \hat{\boldsymbol{I}}^{(t)}}{N - \mathrm{Re}\left\{\boldsymbol{U}\hat{\boldsymbol{I}}^{(t)}\right\}} \right) \right\|^2, \tag{14}$$

$$\rho^{(t+1)} = \left| \frac{\boldsymbol{\mu}\left(\boldsymbol{\eta}^{(t+1)}\right)^H \left(\boldsymbol{x} - A^{(t+1)} \hat{\boldsymbol{I}}^{(t)}\right)}{\boldsymbol{\mu}\left(\boldsymbol{\eta}^{(t+1)}\right)^H \boldsymbol{\mu}\left(\boldsymbol{\eta}^{(t+1)}\right)} \right|, \tag{15}$$

$$\varphi^{(t+1)} = \arg\left(\frac{\boldsymbol{\mu}\left(\boldsymbol{\eta}^{(t+1)}\right)^H \left(\boldsymbol{x} - A^{(t+1)} \hat{\boldsymbol{I}}^{(t)}\right)}{\boldsymbol{\mu}\left(\boldsymbol{\eta}^{(t+1)}\right)^H \boldsymbol{\mu}\left(\boldsymbol{\eta}^{(t+1)}\right)} \right), \tag{16}$$

$$A^{(t+1)} = \frac{\mathrm{Re}\left\{ \left(\hat{\boldsymbol{I}}^{(t)}\right)^H \boldsymbol{\Pi}^\perp_{\boldsymbol{\mu}\left(\boldsymbol{\eta}^{(t+1)}\right)} \boldsymbol{x} \right\}}{N - \mathrm{Re}\left\{ \left(\hat{\boldsymbol{I}}^{(t)}\right)^H \boldsymbol{\Pi}_{\boldsymbol{\mu}\left(\boldsymbol{\eta}^{(t+1)}\right)} \hat{\boldsymbol{I}}^{(t)} \right\}}, \tag{17}$$

$$\begin{aligned} \left(\sigma^2\right)^{(t+1)} = \frac{1}{N} \left\| \boldsymbol{x} - \rho^{(t+1)} e^{j\varphi^{(t+1)}} \boldsymbol{\mu}(\boldsymbol{\eta}^{(t+1)}) - A^{(t+1)} \hat{\boldsymbol{I}}^{(t)} \right\|^2 \\ + \left(A^{(t+1)}\right)^2 \left(1 - \frac{1}{N} \sum_{k=N_1}^{N_2} \left(w_k^{(t)}\right)^2 \right). \end{aligned} \tag{18}$$

[1] $\boldsymbol{\Pi}_{\boldsymbol{A}}$ defines the orthogonal projector onto the column space of $\boldsymbol{A}$, and its complement is $\boldsymbol{\Pi}^\perp_{\boldsymbol{A}} = \mathbf{I} - \boldsymbol{\Pi}_{\boldsymbol{A}}$.

IV. Riemannian Optimization for the E-Step

Each $\tilde{I}_k$ lives on a continuous space given by the complex circle denoted as $\mathcal{S} = \{x \in \mathbb{C} : |x| = 1\}$. The complex circle, $\mathcal{S}$, is a smooth Riemannian sub-manifold of $\mathbb{C}$. The set of N interferences is the Cartesian product of N complex circles, i.e., $\mathcal{S} \times \mathcal{S} \times \cdots \times \mathcal{S}$ (N times). This product of smooth Riemannian manifolds is itself a smooth Riemannian submanifold of $\mathbb{C}^N$, known as the complex circle manifold as described in [14]. The product is formally defined as

$$\mathcal{M} = \left\{ \tilde{\boldsymbol{I}} \in \mathbb{C}^N : \left| \tilde{I}_k \right| = 1 \right\}. \tag{19}$$

A. Background on Riemannian optimization

Manifold optimization is primarily used to mitigate the computational complexity of non-convex constrained optimization problems. By leveraging the geometric properties of the constraints, this transforms the original problem into an unconstrained one. This approach follows the same fundamental steps as classical Euclidean optimization: i) the process begins with an initial point on the manifold, ii) the descent direction is computed at the tangent space of the current point, and iii) the resulting point is then mapped back onto the manifold using an operation known as retraction [14], [16]. More precisely, to optimize an objective function f, and starting from a point $\tilde{\boldsymbol{I}}_\ell^{(t)} \in \mathcal{M}$, where ℓ is the ℓ-th iteration of the gradient descent algorithm, the gradient $\nabla f(\tilde{\boldsymbol{I}}_\ell^{(t)})$ is computed as,

$$\nabla f\left(\tilde{\boldsymbol{I}}_\ell^{(t)}\right) = \left[\cdots, \ \frac{\partial f}{\partial \tilde{I}_k}, \ \cdots \right] \Big|_{\tilde{\boldsymbol{I}} = \tilde{\boldsymbol{I}}_\ell^{(t)}}. \tag{20}$$

But this direction does not necessarily result in an update that remains on $\mathcal{M}$, and one resorts to the tangent space of $\mathcal{M}$ at $\tilde{\boldsymbol{I}}_\ell^{(t)}$, $T_{\tilde{\boldsymbol{I}}_\ell^{(t)}}\mathcal{M}$. The orthogonal projector onto this tangent space is used to project the gradient, yielding the so-called Riemannian gradient, $\nabla_{\mathcal{M}} f\left(\tilde{\boldsymbol{I}}_\ell^{(t)}\right)$, illustrated in Fig. 1.

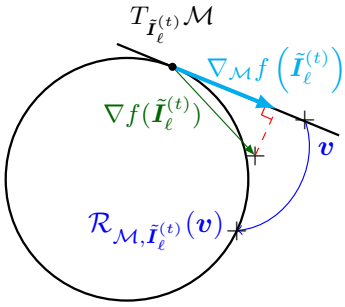

Fig. 1: Illustration of the tangent space of the manifold.

Once the Riemannian gradient is obtained, a direction of descent must be computed to update the algorithm. Following [14], we adopt the Polak-Ribière [17, Chap. 8.3] conjugate gradient algorithm, which defines the descent direction as,

$$\boldsymbol{d}_\ell = -\nabla_{\mathcal{M}} f\left(\tilde{\boldsymbol{I}}_\ell^{(t)}\right) + \beta_\ell \mathcal{T}_{\tilde{\boldsymbol{I}}_{\ell-1}^{(t)} \to \tilde{\boldsymbol{I}}_\ell^{(t)}}(\boldsymbol{d}_{(\ell-1)}), \tag{21}$$

where $\mathcal{T}_{\tilde{\boldsymbol{I}}_{\ell-1}^{(t)} \to \tilde{\boldsymbol{I}}_\ell^{(t)}}(\boldsymbol{d}_{(\ell-1)})$ is referred to as vector transport, and corresponds to the orthogonal projection of the previous descent direction $\boldsymbol{d}_{(\ell-1)}$ onto the current tangent space $T_{\tilde{\boldsymbol{I}}_\ell^{(t)}}\mathcal{M}$. Since $\boldsymbol{d}_{(\ell-1)}$ was originally computed in the previous tangent space $T_{\tilde{\boldsymbol{I}}_{\ell-1}^{(t)}}\mathcal{M}$, this projection ensures consistency in the optimization process. The term β_ℓ is the Polak-Ribière conjugate parameter, given by,

$$\beta_\ell = \nabla f\left(\tilde{\boldsymbol{I}}_\ell^{(t)}\right)^H \frac{\left(\nabla f\left(\tilde{\boldsymbol{I}}_\ell^{(t)}\right) - \mathcal{T}_{\tilde{\boldsymbol{I}}_{\ell-1}^{(t)} \to \tilde{\boldsymbol{I}}_\ell^{(t)}}\left(\nabla f\left(\tilde{\boldsymbol{I}}_{\ell-1}^{(t)}\right)\right)\right)}{\left\|\nabla f\left(\tilde{\boldsymbol{I}}_{\ell-1}^{(t)}\right)\right\|^2}. \tag{22}$$

With the descent direction selected, the next step is to define the step size τ_ℓ. Following [14], we adopt the Armijo backtracking line search algorithm [17, Chap. 4.2]. This method seeks a step that ensures a sufficient decrease in the objective function, as dictated by the Armijo condition. The process begins by testing an initial step size; if it satisfies the condition, it is accepted, otherwise it is progressively reduced until the criterion is met. Finally, an additional step, known as the retraction and denoted $\mathcal{R}_{\mathcal{M},\tilde{\boldsymbol{I}}_\ell^{(t)}}$, is required to map the update back onto the manifold $\mathcal{M}$ from the tangent space $T_{\tilde{\boldsymbol{I}}_\ell^{(t)}}\mathcal{M}$. This is illustrated in Fig. 1, leading to the update

$$\tilde{\boldsymbol{I}}_{\ell+1}^{(t)} = \mathcal{R}_{\mathcal{M},\tilde{\boldsymbol{I}}_\ell^{(t)}}(\tau_\ell \boldsymbol{d}_\ell). \tag{23}$$

B. Proposed approach

We propose to replace the E-step (10) with a Riemannian optimization of the interference phases. To do so, we use the current estimates of the signal parameters $\boldsymbol{\varepsilon}^{(t)}$, leading to,

$$\boldsymbol{x} = \alpha^{(t)} \boldsymbol{\mu}\left(\boldsymbol{\eta}^{(t)}\right) + A^{(t)} \tilde{\boldsymbol{I}}_\ell^{(t)} + \boldsymbol{n}. \tag{24}$$

Defining $\boldsymbol{y}^{(t)} = \boldsymbol{x} - \alpha^{(t)} \boldsymbol{\mu}\left(\boldsymbol{\eta}^{(t)}\right)$, we propose to replace the E-step with the following minimization

$$\underset{\tilde{\boldsymbol{I}}_\ell^{(t)} \in \mathcal{M}}{\arg\min} f\left(\tilde{\boldsymbol{I}}_\ell^{(t)}\right). \tag{25}$$

where the cost function is

$$f\left(\tilde{\boldsymbol{I}}_\ell^{(t)}\right) = \left(\boldsymbol{y}^{(t)} - A^{(t)} \tilde{\boldsymbol{I}}_\ell^{(t)}\right)^H \left(\boldsymbol{y}^{(t)} - A^{(t)} \tilde{\boldsymbol{I}}_\ell^{(t)}\right). \tag{26}$$

Note that (25) has a unique solution since the cost function f in (26) is strongly convex [18, Corollary 1.5, Chap. 6] (the strong convexity can be shown with [18, Theorem 1.2, Chap. 6]). Therefore we are guaranteed to converge to the global minimizer, regardless of the initialization. Starting from a value $\tilde{\boldsymbol{I}}_0^{(t)}$, the gradient of the objective function is

$$\nabla f\left(\tilde{\boldsymbol{I}}_\ell^{(t)}\right) = -2A^{(t)}\left(\boldsymbol{y}^{(t)} - A^{(t)} \tilde{\boldsymbol{I}}_\ell^{(t)}\right). \tag{27}$$

For the manifold (19), the tangent space at $\tilde{\boldsymbol{I}}_\ell^{(t)}$ can be expressed as [14]

$$T_{\tilde{\boldsymbol{I}}_\ell^{(t)}}\mathcal{M} = \left\{ \boldsymbol{v} \in \mathbb{C}^N, \mathrm{Re}\left\{ \boldsymbol{v} \odot \left(\tilde{\boldsymbol{I}}_\ell^{(t)}\right)^* \right\} \odot \tilde{\boldsymbol{I}}_\ell^{(t)} = \boldsymbol{0}_N \right\}, \tag{28}$$

where $\odot$ is the Hadamard (element-wise) product and $\boldsymbol{0}_N$ is the 0 vector of $\mathbb{C}^N$, leading the orthogonal projector

$$\boldsymbol{\Pi}_{T_{\tilde{\boldsymbol{I}}_\ell^{(t)}}\mathcal{M}}(\boldsymbol{v}) = \boldsymbol{v} - \mathrm{Re}\left\{ \boldsymbol{v} \odot \left(\tilde{\boldsymbol{I}}_\ell^{(t)}\right)^* \right\} \odot \tilde{\boldsymbol{I}}_\ell^{(t)}. \tag{29}$$

The Riemannian gradient is obtained by applying (29) to (27)

$$\begin{aligned}&\nabla_{\mathcal{M}} f\left(\tilde{\boldsymbol{I}}_{\ell}^{(t)}\right)\\&\triangleq \nabla f\left(\tilde{\boldsymbol{I}}_{\ell}^{(t)}\right)-\operatorname{Re}\left\{\nabla f\left(\tilde{\boldsymbol{I}}_{\ell}^{(t)}\right)\odot\left(\tilde{\boldsymbol{I}}_{\ell}^{(t)}\right)^{*}\right\}\odot\tilde{\boldsymbol{I}}_{\ell}^{(t)}\\&=-2A^{(t)}\boldsymbol{\Pi}_{T_{\tilde{\boldsymbol{I}}_{\ell}^{(t)}}\mathcal{M}}(\boldsymbol{y}^{(t)}).\end{aligned}\tag{30}$$

The vector transport is

$$\mathcal{T}_{\tilde{\boldsymbol{I}}_{\ell}^{(t-1)}\rightarrow\tilde{\boldsymbol{I}}_{\ell}^{(t)}}\left(\boldsymbol{d}_{(\ell-1)}\right)=\boldsymbol{\Pi}_{T_{\tilde{\boldsymbol{I}}_{\ell}^{(t)}}\mathcal{M}}(\boldsymbol{d}_{(\ell-1)}),\tag{31}$$

and the Polak-Ribière conjugate parameter, using (22) and defining $\boldsymbol{g}_{\ell}^{(t)}=\left(\boldsymbol{y}^{(t)}-A^{(t)}\tilde{\boldsymbol{I}}_{\ell}^{(t)}\right)$, is

$$\beta_{\ell}=\frac{f\left(\tilde{\boldsymbol{I}}_{\ell}^{(t)}\right)-\left(\boldsymbol{g}_{\ell}^{(t)}\right)^{H}\boldsymbol{\Pi}_{T_{\tilde{\boldsymbol{I}}_{\ell}^{(t)}}\mathcal{M}}\left(\boldsymbol{g}_{\ell-1}^{(t)}\right)}{f\left(\tilde{\boldsymbol{I}}_{\ell-1}^{(t)}\right)}.\tag{32}$$

Then, the descent direction yields to (refers to (21))

$$\boldsymbol{d}_{\ell}=\boldsymbol{\Pi}_{T_{\tilde{\boldsymbol{I}}_{\ell}^{(t)}}\mathcal{M}}(2A^{(t)}\boldsymbol{y}^{(t)})+\beta_{\ell}\boldsymbol{\Pi}_{T_{\tilde{\boldsymbol{I}}_{\ell}^{(t)}}\mathcal{M}}(\boldsymbol{d}_{(\ell-1)}).\tag{33}$$

Finally, the retraction is expressed as [14]

$$\mathcal{R}_{\mathcal{M},\tilde{\boldsymbol{I}}_{\ell}^{(t)}}(\boldsymbol{v})=\frac{\tilde{\boldsymbol{I}}_{\ell}^{(t)}+\boldsymbol{v}}{\left\|\tilde{\boldsymbol{I}}_{\ell}^{(t)}+\boldsymbol{v}\right\|},\tag{34}$$

which leads to the update

$$\tilde{\boldsymbol{I}}_{\ell+1}^{(t)}=\frac{\tilde{\boldsymbol{I}}_{\ell}^{(t)}+\tau_{\ell}\boldsymbol{d}_{\ell}}{\left\|\tilde{\boldsymbol{I}}_{\ell}^{(t)}+\tau_{\ell}\boldsymbol{d}_{\ell}\right\|}.\tag{35}$$

All these steps are summarized in Alg. 1.

Algorithm 1 Riemannian Conjugate Gradient Algorithm

1: Initialize $\tilde{\boldsymbol{I}}_{0}^{(t)}$ to a random point on the manifold $\mathcal{M}$;
2: Set $\boldsymbol{d}_0=-\nabla_{\mathcal{M}}f(\tilde{\boldsymbol{I}}_{0}^{(t)})$;
3: $\ell=0$
4: **while** $||-\nabla_{\mathcal{M}}f(\tilde{\boldsymbol{I}}_{\ell}^{(t)})>10^{-3}||$ **do**
5: $\quad\ell\leftarrow\ell+1$
6: $\quad$Compute β_{ℓ} using (32);
7: $\quad$Compute $\boldsymbol{d}_{\ell}$ using (33);
8: $\quad$Compute τ_{ℓ} using [17, Def. 4.2.2];
9: $\quad$Update $\tilde{\boldsymbol{I}}_{\ell+1}$ using (35)
10: **end while**

V. Experimental Results

We consider the scenario in which a GPS L1 C/A signal [19] is attacked by a jammer generating a linear frequency modulated signal, which is defined as:

$$I(t)=\Pi_T(t)\times e^{j\pi\alpha_c t^2+j\phi},\quad \Pi_T(t)=\begin{cases}A & \text{for } 0\le t<T\\ 0 & \text{otherwise}\end{cases}\tag{36}$$

with α_c the chirp rate, A the amplitude and $T=NT_s$ the waveform period. The instantaneous frequency is $f(t)=\frac{1}{2\pi}\frac{d}{dt}(\pi\alpha_c t^2)=\alpha_c t$, and therefore the waveform bandwidth is $B_c=\alpha_c T$. We consider the case where, after the Hilbert filter, the chirp is located at the baseband frequency, i.e., the central chirp frequency is set to 0. Then, the chirp equation is

$$I(t)=\Pi_T(t)\times e^{j\pi\alpha_c(t-T/2)^2+j\phi}.\tag{37}$$

A. Estimation results

The root mean square error (RMSE) of the time-delay parameter τ is illustrated in Fig. 2 with respect to the signal-to-noise ratio at the output of the matched filter (SNR_{OUT}), and considering the following setup: a GNSS receiver with $F_s=4$ MHz, and a chirp bandwidth $B_c=2$ MHz, with initial phase $\phi=0$, amplitude $A=40$ and integration time $T=1$ ms. All results are averaged over 1000 Monte Carlo runs. In the results, we show: a) $\sqrt{\text{CRB}}$, as detailed in [20], which characterizes the asymptotic estimation accuracy of the GNSS parameters in the absence of interference; b) $\sqrt{\text{MCRB}+bias^2}$, as described in [15], which reflects the asymptotic estimation performance in the presence of interference, and represents the asymptotic RMSE of the misspecified MLE (MMLE) [15]; c) the RMSE for the EM algorithm derived in [12]; and d) the RMSE for the EM algorithm with the derivation of the E-step using the Riemannian optimization from Sec. IV. Note that the manifold optimization-based approach outperforms the classical EM method, with the optimization algorithm converging approximately 2 dB earlier. Furthermore, both algorithms are unbiased and can effectively mitigate the interference effects, as the MSE asymptotically approaches the CRB. As a final remark, it should be noted that the initialization of both algorithms uses the MMLE result, as proposed in [12].

For completeness, the Doppler RMSE is given in Fig. 3 with respect to the SNR_{OUT}. We can see again the same effect as for the delay estimation, i.e., convergence at a lower SNR.

B. On the execution time

Simulations were conducted on an Intel(R) Core(TM) i9-10940X processor using MATLAB R2022a. The results are based on the EM algorithm implementation from [12], with optimization carried out using the 'Manopt (7.1)' toolbox [21]. The mean execution time for a single Monte Carlo run is 0.95s for the standard EM [12] and 0.75s for the manifold optimization-based EM, i.e., the standard EM algorithm nearly doubles the execution time. This is primarily due to the standard E-step that involves the use of modified Bessel functions. Then, replacing this step with the Riemannian optimization leads to a significant reduction in computational time.

VI. Conclusion

In this work, we introduced a novel EM algorithm in which the E-step leverages Riemannian optimization. This approach significantly improves the convergence in terms of MSE for the time-delay estimation, as the algorithm converges 2 dB earlier compared to the standard EM method. Additionally, by avoiding the use of modified Bessel functions in the E-step, this method substantially reduces execution time, enhancing computational efficiency. Through simulations, we

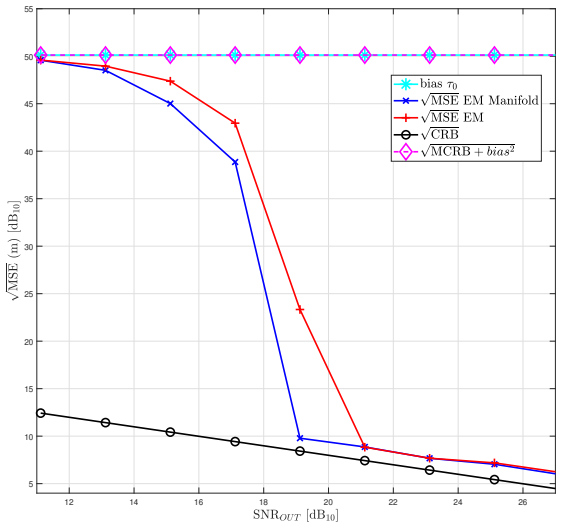

Fig. 2: Time-delay RMSE for a GPS L1 C/A signal corrupted by a linear chirp signal.

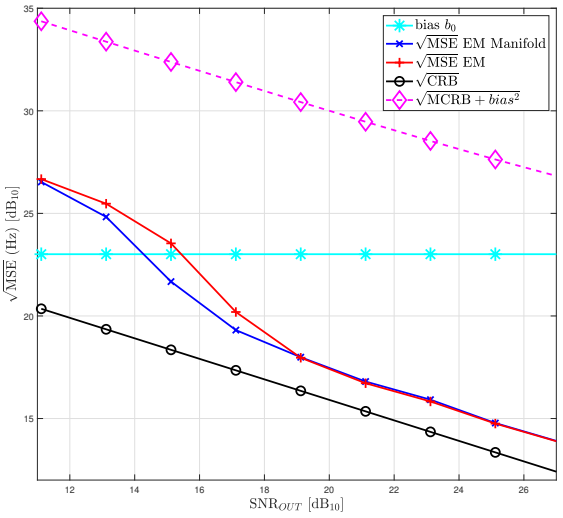

Fig. 3: Doppler RMSE for a GPS L1 C/A signal corrupted by a linear chirp signal.

demonstrated the effectiveness of the proposed algorithm in estimating GNSS parameters in the presence of chirp interference jamming. These results highlight the potential of Riemannian optimization for improving GNSS signal processing in interference environments. Future work is to consider more complex interference scenarios and real-world GNSS datasets.

REFERENCES

[1] M. G. Amin, P. Closas, A. Broumandan, and J. L. Volakis, "Vulnerabilities, Threats, and Authentication in Satellite-based Navigation Systems [scanning the issue]," *Proceedings of the IEEE*, vol. 104, no. 6, pp. 1169–1173, June 2016.

[2] F. Dovis, *GNSS Interference Threats & Countermeasures*. Artech House, 2015.

[3] E. Kaplan and C. Hegarty, *Understanding GPS: Principles And Applications*, 11 2005.

[4] C. Fernández-Prades, J. Arribas, and P. Closas, "Robust GNSS receivers by array signal processing: Theory and implementation," *Proceedings of the IEEE*, vol. 104, no. 6, pp. 1207–1220, June 2016.

[5] D. Borio and P. Closas, "A Fresh Look at GNSS Anti-Jamming," *InsideGNSS*, pp. 54–61, September/October 2017.

[6] D. Borio, "Swept GNSS Jamming Mitigation Through Pulse Blanking," in *Proc. 2016 European Navigation Conference (ENC)*, Helsinki, Finland, Aug. 2016, pp. 1–8.

[7] D. Borio, C. O'Driscoll, and J. Fortuny, "Tracking and Mitigating a Jamming Signal with an Adaptive Notch Filter," *InsideGNSS*, pp. 67–73, March/April 2014.

[8] H. Elghamrawy, M. Karaim, M. Korenberg, and A. Noureldin, "High-Resolution Spectral Estimation for Continuous Wave Jamming Mitigation of GNSS Signals in Autonomous Vehicles," *IEEE Trans. Intell. Transp. Syst.*, vol. 23, no. 7, pp. 7881–7895, 2022.

[9] I. E. Mehr and F. Dovis, "A Deep Neural Network Approach for Classification of GNSS Interference and Jammer," *IEEE Trans. Aerosp. Electron. Syst.*, pp. 1–18, 2024.

[10] D. Borio and C. C. Gioia, "GNSS Interference Mitigation: A Measurement and Position Domain Assessment," vol. 68, no. 1, pp. 93–114, 2021.

[11] H. Li, S. Tang, P. Wu, and P. Closas, "Robust Interference Mitigation Techniques for Direct Position Estimation," *IEEE Transactions on Aerospace and Electronic Systems*, vol. 59, no. 6, pp. 8969–8980, 2023.

[12] J. Lesouple and L. Ortega, "An EM Approach for GNSS Parameters of Interest Estimation Under Constant Modulus Interference," in *2023 31st European Signal Processing Conference (EUSIPCO)*, 2023, pp. 820–824.

[13] ——, "Bayesian EM approach for GNSS parameters of interest estimation under constant modulus interference," *EURASIP Journal on Advances in Signal Processing*, vol. 2024, no. 1, p. 32, Mar. 2024.

[14] M. ElMossallamy, K. Seddik, W. Chen, L. Wang, G. Li, and Z. Han, "RIS Optimization on the Complex Circle Manifold for Interference Mitigation in Interference Channels," *IEEE Transactions on Vehicular Technology*, vol. 70, no. 6, pp. 6184–6189, 2021.

[15] L. Ortega, C. Lubeigt, J. Vilà-Valls, and E. Chaumette, "On GNSS Synchronization Performance Degradation under Interference Scenarios: Bias and Misspecified Cramér-Rao Bounds," *NAVIGATION: Journal of the Institute of Navigation*, vol. 70, no. 4, 2023.

[16] N. Boumal, P.-A. Absil, and C. Cartis, "Global rates of convergence for nonconvex optimization on manifolds," *IMA Journal of Numerical Analysis*, vol. 39, no. 1, p. 1–33, Feb. 2018. [Online]. Available: http://dx.doi.org/10.1093/imanum/drx080

[17] R. S. P.-A. Absil, R. Mahony, *Optimization Algorithms on Matrix Manifolds*. Princeton University Press.

[18] C. Udriste, *Convex Functions and Optimization Methods on Riemannian Manifolds*. Springer-Science+Business Media, BV.

[19] P. J. Teunissen and O. Montenbruck, *Springer Handbook of Global Navigation Satellite Systems*, 1st ed. Springer Cham, 2017.

[20] D. Medina, L. Ortega, J. Vilà-Valls, P. Closas, F. Vincent, and E. Chaumette, "Compact CRB for Delay, Doppler, and Phase Estimation – Application to GNSS SPP and RTK Performance Characterisation," *IET Radar Sonar and Navigation*, vol. 14, no. 10, pp. 1537–1549, 2020. [Online]. Available: https://hal.science/hal-02974914

[21] N. Boumal, B. Mishra, P.-A. Absil, and R. Sepulchre, "Manopt, a Matlab toolbox for optimization on manifolds," *Journal of Machine Learning Research*, vol. 15, no. 42, pp. 1455–1459, 2014. [Online]. Available: https://www.manopt.org